

Theoretical Study of [2 + 1] Cycloaddition of CO and CS to Acetylenes Forming Cyclopropenones and Cyclopropenethiones

Loc Thanh Nguyen,^{†,‡} Frank De Proft,[‡] Minh Tho Nguyen,^{*,§} and Paul Geerlings^{*,‡}

Faculty of Chemical Engineering, HoChiMinh City University of Technology, HoChiMinh City, Vietnam, Eenheid Algemene Chemie, Vrije Universiteit Brussel, Pleinlaan 2, B-1050 Brussels, Belgium, and Department of Chemistry, University of Leuven, Celestijnenlaan 200F, B-3001 Leuven, Belgium

pgeerlin@vub.ac.be

Received February 20, 2001

The [2 + 1] cycloadditions of carbon monoxide and carbon monothiooxide CX (X = O, S) to acetylenes (R₁C≡CR₂ with R₁ = H, OH and R₂ = CH₃, OH, NH₂, C₆H₅) have been studied at the B3LYP/6-311G(d,p) level. It has been shown that the reaction proceeds in two steps forming first an intermediate having the properties of both a carbene and a zwitterion followed by a ring closure leading to cyclopropenones or cyclopropenethiones. The solvent effect does not play an important role in the course of the cycloaddition. The estimation of the first vertical excitation energies by CIS and TD-B3LYP methods shows that the reactions likely take place in the ground state rather than in an excited state. All the studied cyclopropenones and cyclopropenethiones are aromatic as shown by their NICS values and confirmed by calculated and experimental NMR chemical shifts. Different reactivity criteria including HOMO coefficient, local softness, hardness, polarizability, and NICS are used to predict the site selectivity in all studied cases, and the NICS criterion seems to yield the best results among them.

Introduction

The first cyclopropenone, diphenylcyclopropenone, was synthesized in 1959.^{1a,b} Until 1963, several methods were used to synthesize this substance, but the best procedure² was the elimination of HBr from α,α' -dibromodibenzyl ketone. Some physicochemical properties and reactions of diphenylcyclopropenone have also been reported since then.^{3–8}

Following the synthesis of diphenylcyclopropenone, a number of other substituted cyclopropenones have been prepared.^{9–11} In 1966, Breslow et al.^{12a} used a new procedure, namely the reaction of lithium trichloromethide at –100 °C with various acetylenes, to produce methyl cyclopropenone and related compounds after a number of attempts to synthesize such compounds from HBr elimination failed. A large number of publications

on the synthesis and physicochemical properties of other substituted cyclopropenones have also been reported, such as diaminocyclopropenones,^{13,20} fluorocyclopropenone,^{14,20} phenylaminocyclopropenones,^{15–17} phenylhydroxycyclopropenone,^{10a,b,18} and hydroxycyclopropenone.^{19,20}

Cyclopropenones have also received considerable attention from theoretical chemists mainly due to their possible description as aromatic compounds. Although aromaticity is important in chemistry, its definition is not unambiguous yet, and a variety of definitions have been proposed.²¹ Among them, those based on magnetic criteria have widely been applied such as magnetic susceptibility exaltations,²² magnetic susceptibility

[†] HoChiMinh City University of Technology.

[‡] Vrije Universiteit Brussel.

[§] University of Leuven. E-mail: minh.nguyen@chem.kuleuven.ac.be

(1) (a) Volpin, M. E.; Koreshkov, Yu. D.; Kursanov, D. N. *Izv. Akad. Nauk SSSR, Otd. Khim. Nauk* **1959**, 560. (b) Breslow, R.; Haynie, R.; Mirra, J. *J. Am. Chem. Soc.* **1959**, 81, 247.

(2) Breslow, R.; Posner, J.; Krebs, A. *J. Am. Chem. Soc.* **1963**, 85, 234.

(3) Breslow, R.; Eicher, T.; Krebs, A.; Peterson, R. A.; Posner, J. *J. Am. Chem. Soc.* **1965**, 87, 1320.

(4) Ammon, H. L. *J. Am. Chem. Soc.* **1973**, 95, 7093.

(5) Hopkins, H. P., Jr.; Bostwick, D.; Alexander, C. J. *J. Am. Chem. Soc.* **1976**, 98, 1355.

(6) Müller, C.; Schweig, A.; Vermeer, H. *J. Am. Chem. Soc.* **1978**, 100, 8056.

(7) Greenberg, A.; Tomkins, R. P. T.; Dobrovolny, M.; Liebman, J. *J. Am. Chem. Soc.* **1983**, 105, 6855.

(8) Grabowski, J. J.; Simon, J. D.; Peters, K. S. *J. Am. Chem. Soc.* **1984**, 106, 4615.

(9) Breslow, R.; Peterson, R. *J. Am. Chem. Soc.* **1960**, 82, 4426.

(10) (a) Farnum, D. G.; Thurston, P. E. *J. Am. Chem. Soc.* **1964**, 86, 4206. (b) Chickos, J. S.; Patton, E.; West, R. *J. Org. Chem.* **1974**, 39, 1647.

(11) Breslow, R.; Altman, L. J.; Krebs, A.; Mohacsi, E.; Murata, I.; Peterson, R. A.; Posner, J. *J. Am. Chem. Soc.* **1965**, 87, 1326.

(12) (a) Breslow, R.; Altman, L. J. *J. Am. Chem. Soc.* **1966**, 88, 504.

(b) Breslow, R.; Ryan, G. *J. Am. Chem. Soc.* **1967**, 89, 3073. (c) Breslow, R.; Ryan, G.; Groves, J. T. *J. Am. Chem. Soc.* **1970**, 92, 988. (d) Pretsch, E.; Clerk, T.; Seibl, J.; Simon, W. In *Tables for Structure Determination of Organic Compounds by Spectroscopic Techniques* (Chemical Laboratory Practice); Boschke, F. L., Fresenius, W., Huber, J. F. K., Pungor, E., Rehnitz, G. A., Simon, W., West, Th. S., Eds.; Springer-Verlag: Berlin, 1983.

(13) Yoshida, Z.; Konishi, H.; Tawara, Y.; Ogoshi, H. *J. Am. Chem. Soc.* **1973**, 95, 3043.

(14) Dailey, W. P. *J. Org. Chem.* **1995**, 60, 6737.

(15) Andraos, J.; Chiang, Y.; Grant, A. S.; Guo, H.-X.; Kresge, A. J. *J. Am. Chem. Soc.* **1994**, 116, 7411.

(16) Chiang, Y.; Grant, A. S.; Kresge, A. J.; Paine, S. W. *J. Am. Chem. Soc.* **1996**, 118, 4366.

(17) Chiang, Y.; Grant, A. S.; Guo, H.-X.; Kresge, A. J.; Paine, S. W. *J. Org. Chem.* **1997**, 62, 5363.

(18) Chiang, Y.; Kresge, A. J.; Hochstrasser, R.; Wirz, J. *J. Am. Chem. Soc.* **1989**, 111, 2355.

(19) Chiang, Y.; Kresge, A. J.; Popik, V. V. *J. Am. Chem. Soc.* **1995**, 117, 9165.

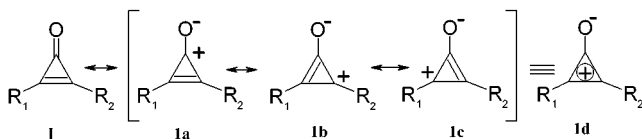
(20) Sung, K.; Fang, D.; Glenn, D.; Tidwell, T. T. *J. Chem. Soc., Perkin Trans. 2* **1998**, 2073.

(21) (a) Schleyer, P. v. R.; Jiao, H. *Pure Appl. Chem.* **1996**, 68, 209 and references therein. (b) Krygowski, T. M.; Cyrański, M. K.; Czarnocki, Z.; Häfelinger, G.; Katritzky, A. R. *Tetrahedron* **2000**, 56, 1783.

(22) Schleyer, P. v. R.; Freeman, P.; Jiao, H.; Goldfuss, B. *Angew. Chem., Int. Ed. Engl.* **1995**, 34, 337.

anisotropies,^{22,23} or more recently, nucleus-independent chemical shifts (NICS).²⁴ Generally, for aromatic compounds, large magnetic susceptibility exaltations and anisotropies, as well as large negative NICS values, are attributed to cyclic π -electron delocalization.²⁵

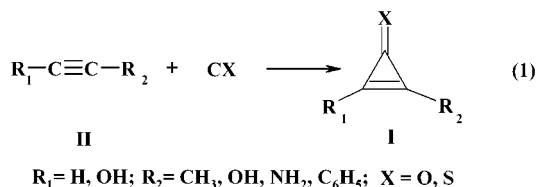
Cyclopropenones were first proposed to be aromatic in the work of Manatt et al.²⁶ and Breslow et al.^{1b} in 1959. These systems can be represented by the resonance structures **1a–c** (equivalent to **1d**),^{20,27} which contain a three-membered ring of sp^2 carbons coupled two exocyclic π electrons, and it appears that electron-donor substituents seem to stabilize these structures.



Until now, the question if cyclopropenones are aromatic has not been clearly answered. Some authors suggested that cyclopropenones are aromatic or moderately aromatic,^{1b,3,7,8,11,27–33} whereas others^{34,35} concluded that they are not aromatic at all. Therefore, the work of verifying the aromaticity of cyclopropenones is still valuable. The question also rises to which extent aromaticity and its evolution upon reaction influence the reactivity of cyclopropenones. Proceeding in the opposite direction, the [2 + 1] cycloaddition of CX (X = O, S) to acetylenes has been studied in our recent preliminary work.³⁶ It turns out that the addition is stepwise, forming cyclopropenone and cyclopropenethione via an intermediate. The intermediate has the properties of a semi-carbene, semi-zwitterion, and its structure is best described in both cases as a resonance hybrid between a carbene and a zwitterion.

In an attempt to determine if the results obtained in the previous work³⁶ could be generalized and in relation with our recent theoretical studies on using reactivity descriptors based on the density functional theory (DFT) in studying the regioisomeric mechanism^{37–42} and aroma-

ticity,^{43a,b} we have carried out quantum chemical calculations on the additions with the substituents listed in eq 1.



We thus analyze the mechanistic aspects, in particular the regioisomeric mechanism and asynchronism, by using the DFT-based reactivity descriptors and the nucleus-independent chemical shift (NICS) criteria. Besides, to investigate if all the reactions take place in the ground state rather than in an excited state as required in the flash photolytic techniques^{15–20,27,28} and to study the solvent effect on this kind of reactions, the first vertical excitation energies and the solvent effect in three typical solvents that have different dielectric constants (water, acetonitrile, and benzene) have also been probed in one case, namely phenylhydroxycyclopropenone (R_1 = phenyl and R_2 = OH), which is the derivative most extensively studied experimentally.

Methods of Calculation

Calculations were performed using the Gaussian 98 suite of programs.^{44a} All structures were fully optimized with the hybrid-exchange correlation B3LYP functional and a 6-311G-(d,p) basis set. Zero-point vibrational energies (ZPEs) were calculated at the B3LYP/6-311G(d,p) level and scaled down by a factor of 0.98.^{44b} The choice of substituents provides a representative survey of several of the most important types encountered in practice. To verify the connectivity of transition structures with reactants and products, the intrinsic reaction coordinate (IRC) calculations have been carried out at the B3LYP/6-311G(d,p) level. Atomic charges were taken from electrostatic potential driven (ESP) and natural population analysis (NPA) by using the MK and NPA options in the Gaussian program. The first vertical excitation energies were

- (23) Benson, R. C.; Flygare, W. H. *J. Am. Chem. Soc.* **1970**, *92*, 7523.
 (24) (a) Schleyer, P. v. R.; Maerker, C.; Dransfeld, A.; Jiao, H.; van Eikema Hommes, N. J. R. *J. Am. Chem. Soc.* **1996**, *118*, 6317. (b) Schleyer, P. v. R.; Jiao, H.; van Eikema Hommes, N. J. R.; Malkin, V. G.; Malkina, O. L. *J. Am. Chem. Soc.* **1997**, *119*, 12699. (c) West, R.; Buffy, J. J.; Haaf, M.; Müller, T.; Gehrhus, B.; Lappert, M.; Apeloig, Y. *J. Am. Chem. Soc.* **1998**, *120*, 1639.
 (25) Morao, I.; Cossio, F. P. *J. Org. Chem.* **1999**, *64*, 1868.
 (26) Manatt, S. L.; Roberts, J. D. *J. Org. Chem.* **1959**, *24*, 1336.
 (27) Staley, S. W.; Norden, T. D.; Taylor, W. H.; Harmony, M. D. *J. Am. Chem. Soc.* **1987**, *109*, 7641.
 (28) Benson, R. C.; Flygare, W. H.; Oda, M.; Breslow, R. *J. Am. Chem. Soc.* **1973**, *95*, 2772.
 (29) Krebs, A. W. *Angew. Chem., Int. Ed. Engl.* **1965**, *4*, 10.
 (30) Dahn, H.; Ung-Truong, M. N. *Helv. Chim. Acta* **1987**, *70*, 2130.
 (31) Budzelaar, P. H.; Kraka, E.; Cremer, D.; Schleyer, P. v. R. *J. Am. Chem. Soc.* **1986**, *108*, 561.
 (32) Hase, H. L.; Muller, C.; Schweig, A. *Tetrahedron* **1978**, *34*, 2893.
 (33) (a) Ammon, H. L. *J. Am. Chem. Soc.* **1973**, *95*, 7093. (b) Schäfer, W.; Schweig, A. *Tetrahedron Lett.* **1974**, 1213. (c) Yamabe, S.; Morokuma, K. *J. Am. Chem. Soc.* **1975**, *97*, 4458. (d) Grier, D. L.; Streitwieser, A., Jr. *J. Am. Chem. Soc.* **1982**, *104*, 3556.
 (34) Fitzpatrick, J. N.; Fanning, M. O. *J. Mol. Struct.* **1975**, *25*, 197.
 (35) (a) Pitman, C. U., Jr.; Kress, A.; Patterson, T. B.; Walton, P.; Kispert, L. D. *J. Org. Chem.* **1974**, *39*, 373. (b) Scancke, A. *J. Mol. Struct.* **1976**, *30*, 95.
 (36) Nguyen, L. T.; De Proft, F.; Nguyen, M. T.; Geerlings, P. *J. Chem. Soc., Perkin Trans. 2*, in press.
 (37) (a) Nguyen, L. T.; Le, T. N.; De Proft, F.; Chandra, A. K.; Langenaeker, W.; Nguyen, M. T.; Geerlings, P. *J. Am. Chem. Soc.* **1999**, *121*, 5992. (b) T. N. Le, L. T. Nguyen, A. K. Chandra, F. De Proft, P. Geerlings, M. T. Nguyen, *J. Chem. Soc., Perkin Trans. 2*, **1999**, 1249.

- (38) Nguyen, M. T.; Vansweevelt, H.; Vanquickenborne, L. G. *J. Org. Chem.* **1991**, *56*, 5651.
 (39) Nguyen, M. T.; Vansweevelt, H.; De Neef, A.; Vanquickenborne, L. G. *J. Org. Chem.* **1994**, *59*, 8015.
 (40) Nguyen, M. T.; Van Keer, A.; Pierloot, K.; Vanquickenborne, L. G. *J. Am. Chem. Soc.* **1995**, *117*, 7535.
 (41) Nguyen, M. T.; Van Keer, A.; Vanquickenborne, L. G. *Chem. Ber./Recl.* **1997**, *130*, 69; *J. Chem. Soc., Perkin Trans. 2* **1996**, 299.
 (42) (a) Chandra, A. K.; Geerlings, P.; Nguyen, M. T. *J. Org. Chem.* **1997**, *62*, 6417. (b) Damoun, S.; Van De Woude, G.; Méndez, F.; Geerlings, P. *J. Phys. Chem. A* **1997**, *101*, 886. (c) Damoun, S.; Van De Woude, G.; Choho, K.; Geerlings, P. *J. Phys. Chem. A* **1999**, *103*, 7861. (d) Roy, R. K.; De Proft, F.; Geerlings, P. *J. Phys. Chem. A* **1998**, *102*, 7035.
 (43) (a) Manoharan, M.; De Proft, F.; Geerlings, P. *J. Chem. Soc., Perkin Trans. 2* **2000**, 1767; *J. Org. Chem.* **2000**, *65*, 7971; *J. Org. Chem.* **2000**, *65*, 6132. (b) De Proft, F.; Geerlings, P. *Chem. Rev.* **2001**, *101*(5), 1451.
 (44) (a) Frisch, M. J.; Trucks, G. W.; Schlegel, H. B.; Scuseria, G. E.; Robb, M. A.; Cheeseman, J. R.; Zakrzewski, V. G.; Montgomery, J. A., Jr.; Stratmann, R. E.; Burant, J. C.; Dapprich, S.; Millam, J. M.; Daniels, A. D.; Kudin, K. N.; Strain, M. C.; Farkas, O.; Tomasi, J.; Barone, V.; Cossi, M.; Cammi, R.; Mennucci, B.; Pomelli, C.; Adamo, C.; Clifford, S.; Ochterski, J.; Petersson, G. A.; Ayala, P. Y.; Cui, Q.; Morokuma, K.; Malick, D. K.; Rabuck, A. D.; Raghavachari, K.; Foresman, J. B.; Cioslowski, J.; Ortiz, J. V.; Stefanov, B. B.; Liu, G.; Liashenko, A.; Piskorz, P.; Komaromi, I.; Gomperts, R.; Martin, R. L.; Fox, D. J.; Keith, T.; Al-Laham, M. A.; Peng, C. Y.; Nanayakkara, A.; Gonzalez, C.; Challacombe, M.; Gill, P. M. W.; Johnson, B. G.; Chen, W.; Wong, M. W.; Andres, J. L.; Head-Gordon, M.; Replogle, E. S.; Pople, J. A. *Gaussian 98*, revision A.7; Gaussian, Inc.: Pittsburgh, PA, 1998. (b) A. P. Scott, L. Radom, *J. Phys. Chem.* **1996**, *100*, 16502. (c) V. Barone, M. Cossi, J. Tomasi, *J. Comput. Chem.* **1998**, *19*, 404.

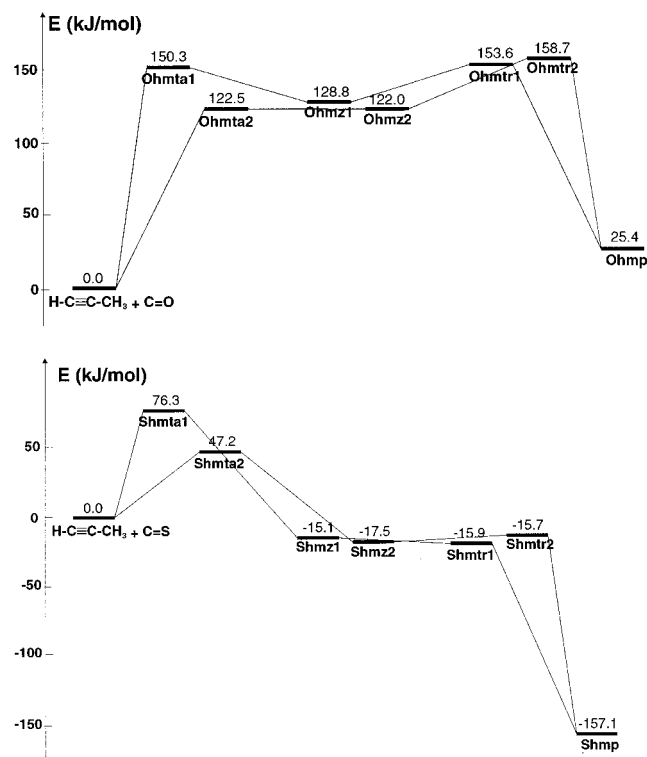


Figure 1. Schematic potential energy profiles for the two-step addition of CX ($X = \text{O}, \text{S}$) to $\text{HC}\equiv\text{CCH}_3$. Relative energies obtained at B3LYP/6-311G(d,p) using B3LYP/6-311G(d,p)-optimized geometries and corrected for zero-point contributions.

estimated by using the configuration interaction including only single-excitations CIS/6-311++G(d,p) and time-dependent density functional theory (TD-B3LYP/6-311++G(d,p)) method. The solvent effect has been probed with the polarizable continuum model (PCM)^{44c} using the SCRF keyword in the Gaussian program. The dielectric constants were taken equal to 78.39 for water, 36.64 for acetonitrile, and 2.247 for benzene. The nucleus-independent chemical shifts (NICS) values were derived from magnetic shieldings computed using the gauge-independent atomic orbital (GIAO) method and using the NMR option in the Gaussian program. In this paper, bond distances are given in angstroms, bond angles in degrees, total energies in hartrees, and zero-point and relative energies in kilojoules per mole.

Results and Discussion

There are a large number of results needed for the discussion, but for the sake of brevity, we have put some of the figures in the Supporting Information. The potential energy surfaces including the zero-point energy corrections for the addition of CX ($X = \text{O}, \text{S}$) to $\text{R}_1\text{C}\equiv\text{CR}_2$ ($\text{R}_1 = \text{H}, \text{R}_2 = \text{CH}_3, \text{OH}, \text{NH}_2, \text{C}_6\text{H}_5$ and $\text{R}_1 = \text{OH}, \text{R}_2 = \text{CH}_3, \text{C}_6\text{H}_5$) are shown in Figures 1 and 5–9. The geometrical parameters of the equilibrium and transition structures (Ts) along the reaction paths are presented in Figures 2 and 3 for the reaction of $\text{CX} + \text{HC}\equiv\text{CCH}_3$. On the basis of our experience on the trans-bending mode of acetylenes when undergoing cycloaddition reactions,^{36,37a} we chose the *Z* conformation when locating the transition-state structure of the addition step. Complete flexibility was given during optimization yielding in most cases the *Z* conformation for the Ts at the B3LYP level, even though in some cases the *E* conformation was obtained at the HF level. The geometries along the reaction path for other reactions are provided as Supporting Information (Figures S1–S10). The highest occupied molecular orbitals (HOMO) of all intermediates in the reaction of $\text{CO} + \text{R}_1\text{C}\equiv\text{CR}_2$ are illustrated in Figure 4.

Classification of the Reactants as Nucleophile or Electrophile. For the purpose of explaining the regioisomeric mechanism with the DFT reactivity descriptors in the [2 + 1] cycloaddition of CX ($X = \text{O}, \text{S}$) to acetylenes, we first need to classify the reactants as either electrophile or nucleophile. Table 1 presents the LUMO – HOMO energy gap and the differences in vertical ionization energies (IE) and electron affinities (EA) for CX ($X = \text{O}, \text{S}$) and acetylenes (R).

It turns out that, in all cases, the energy gaps of $\text{LUMO}_{\text{CX}} - \text{HOMO}_{\text{R}}$ are smaller than those of $\text{LUMO}_{\text{R}} - \text{HOMO}_{\text{CX}}$, as also confirmed by the differences between IE and EA. As such, according to the frontier orbital theory, the CX ($X = \text{O}, \text{S}$) moiety behaves as an electrophilic reagent and acetylenes (R) behave as a nucleophilic reagent. This is in the same vein with the results obtained in the previous work.³⁶ Note that, in the present case, there is an attack of a π -electron pair of acetylenes on the LUMO of CX, acetylenes thus serving as a bond donor as illustrated in the scheme below, followed by a back-donation of CO via the carbon lone pair. This discussion indicates that the regioisomeric mechanism

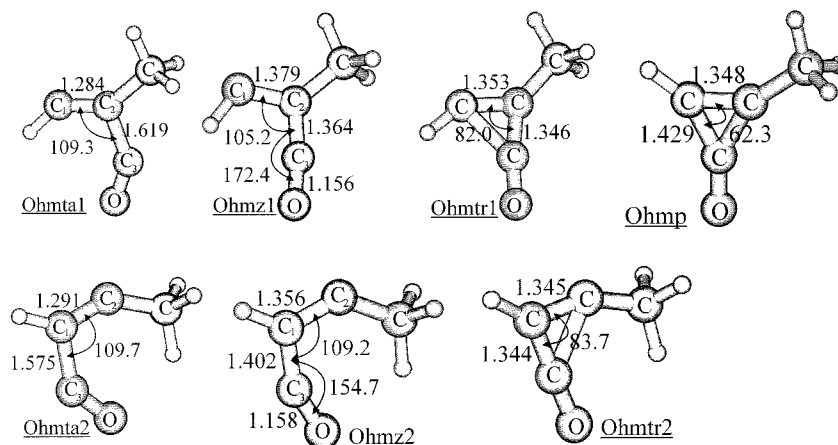
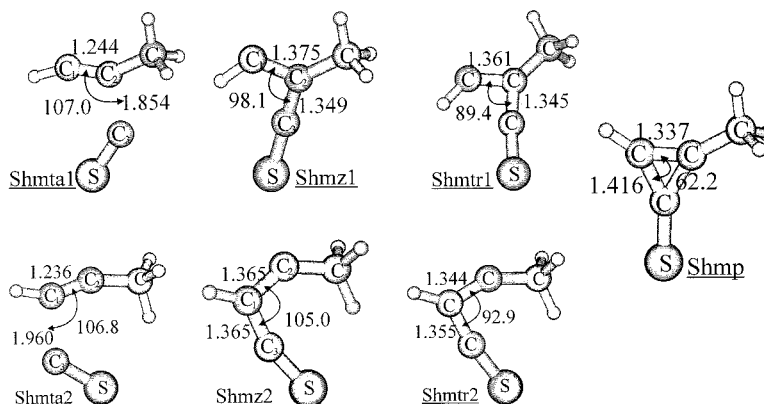


Figure 2. B3LYP/6-311G(d,p) geometrical parameters of the equilibrium and transition structures of the addition of CO to $\text{HC}\equiv\text{CCH}_3$.

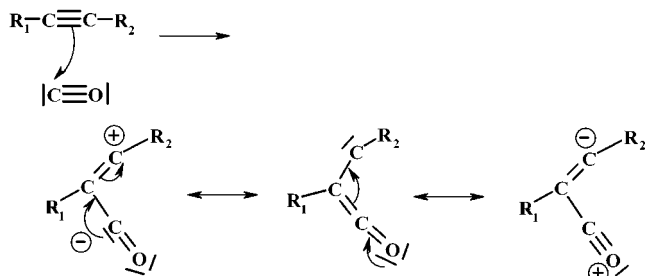
Table 1. Differences (in eV) in LUMO–HOMO Energies and (IE – EA) of CX (X = O, S) and Substituted Acetylenes (R)

structure	E_{LUMO}^a and EA ^b	E_{HOMO}^a and IE ^b	$E_{\text{LUMO}}(\text{R}) - E_{\text{HOMO}}(\text{CO})^a$ and IE(CO) – EA(R) ^b	$E_{\text{LUMO}}(\text{CO}) - E_{\text{HOMO}}(\text{R})^a$ and IE(R) – EA(CO) ^b	$E_{\text{LUMO}}(\text{R}) - E_{\text{HOMO}}(\text{CS})^a$ and IE(CS) – EA(R) ^b	$E_{\text{LUMO}}(\text{CS}) - E_{\text{HOMO}}(\text{R})^a$ and IE(R) – EA(CS) ^b
CO	4.4	-14.9				
	<i>-2.6</i>	<i>14.2</i>				
CS	1.9	-12.5				
	<i>-0.3</i>	<i>11.5</i>				
HC≡CCH ₃	6.1	-10.3	21.0	14.7	18.6	12.2
	<i>-3.0</i>	<i>10.3</i>	<i>17.1</i>	<i>12.9</i>	<i>14.5</i>	<i>10.6</i>
HC≡COH	5.2	-10.1	20.1	14.5	17.7	12.0
	<i>-2.3</i>	<i>10.0</i>	<i>16.4</i>	<i>12.6</i>	<i>13.8</i>	<i>10.3</i>
HC≡CNH ₂	5.8	-9.2	20.7	13.6	18.3	11.1
	<i>-2.6</i>	<i>9.0</i>	<i>16.7</i>	<i>11.6</i>	<i>14.1</i>	<i>9.3</i>
HC≡CC ₆ H ₅	2.9	-8.5	17.8	12.9	15.4	10.5
	<i>-0.8</i>	<i>8.6</i>	<i>15.0</i>	<i>11.2</i>	<i>12.3</i>	<i>8.9</i>
HOC≡CCH ₃	5.5	-9.5	20.4	13.9	18.0	11.4
	<i>-2.4</i>	<i>9.2</i>	<i>16.5</i>	<i>11.8</i>	<i>13.9</i>	<i>9.4</i>
HOC≡CC ₆ H ₅	3.3	-8.1	18.2	12.5	15.8	10.0
	<i>-1.2</i>	<i>8.0</i>	<i>15.4</i>	<i>10.6</i>	<i>12.8</i>	<i>8.2</i>

^a Frontier orbital energies taken from HF/6-31G(d) wave functions (in bold). ^b Vertical ionization energies and electron affinities obtained from B3LYP/6-311G(d,p) computations (in italic).

**Figure 3.** B3LYP/6-311G(d,p) geometries along the reaction path in the reaction of HC≡CCH₃ + CS.

in these reactions can be expected to be governed by the frontier MOs or their generalized DFT counterparts (fukui function, local softness) and not by atomic charges (vide infra).



Potential Energy Surfaces. Reaction of HC≡CCH₃ with CX (X = O, S). Let us begin with the attack of CX (X = O, S) on HC≡CCH₃. The structures shown in Figure 1 include **Xhmta1**, **Xhmta2**, **Xhmz1**, **Xhmz2**, **Xhmtr1**, **Xhmtr2**, and **Xhmp** (X = O, S). The separated systems (CX + HC≡CCH₃) are omitted for simplicity. In general, the structures are labeled by a combination of letters, in which **O** stands for X = O, **S** for X = S, **h** for R₁ = H, **m** for R₂ = CH₃, **t** for transition state, **a** for addition, **r** for ring closure, **z** for intermediate, and **p** for the three-membered ring. In this case, the two acetylene carbon centers are not equivalent, leading to a site

selectivity for the initial attack of CX (X = O, S) to HC≡CCH₃. The label **1** stands for the attack of CX to the substituted carbon of acetylenes and **2** for the attack to the unsubstituted carbon.

As illustrated in Figure 1, the attack of CX to the unsubstituted carbon via the transition state **Xhmta2** is more favorable than that to the substituted center via **Xhmta1**. The latter is about 27 kJ/mol (X = O) and 29 kJ/mol (X = S) higher in energy than the former. The addition turns out to be a two-step process in which the rate-determining step is the ring closure in the CO case, but it is the initial addition in the CS case. The difference is due to the high exothermicity in the formation of cyclopropanethione. Owing to the high stability of carbon monoxide, its cycloaddition is slightly endothermic. Although the addition to the unsubstituted carbon is favored, the corresponding second ring-closure step is less favored. Both additions appear to be competitive processes. Moreover, it is also of interest to notice that the intermediates **Ohmz1**, **Ohmz2**, and **Shmz2** are located in a shallow potential well, whereas **Shmz1** lies a few hundreds joules per mole higher in energy than the transition structure for ring-closure **Shmtr1** after zero-point corrections. Therefore, the intermediates in the CS-case are not observable or even do not exist as discrete points on the potential energy surface if higher level calculations could be performed.

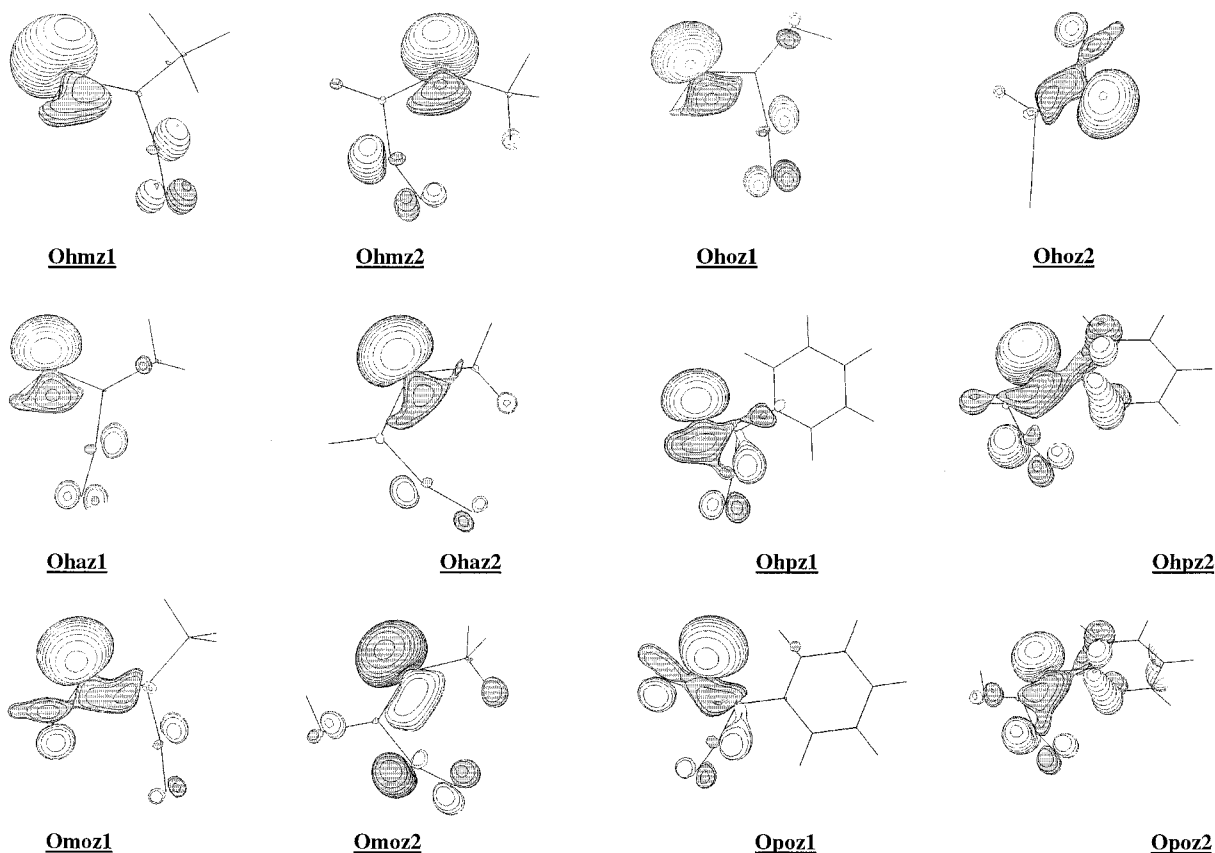


Figure 4. Highest occupied molecular orbitals of the intermediates in the reaction of $\text{CO} + \text{R}_1\text{C}=\text{CR}_2$.

Compared with the intermediates **Xhzh** in the addition of CX (X = O, S) to acetylene $\text{HC}\equiv\text{CH}$,³⁶ it follows from Figure 2 that the carbon–carbon, carbon–oxygen bond distances in the intermediate **Ohmz1** are the same as those in **Ohhz**. In **Ohmz2**, the $\text{C}_1\text{--C}_2$ bond distance is shorter whereas the $\text{C}_2\text{--C}_3$ one is longer than those in **Ohhz** (1.36 and 1.40 Å versus 1.38 and 1.36 Å). Therefore, it is reasonable to propose that **Ohmz1** is still a semi-carbene, semi-zwitterion but **Ohmz2** is rather a zwitterion. Nevertheless, the HOMOs of **Ohmz1** and **Ohmz2** are σ orbitals (Figure 4) and look the same as that in the **Ohhz**. As such, both intermediates still have the properties of a singlet carbene. The geometrical parameters of **Shmz1**, **Shmz2** in Figure 3 show that those structures also have the character of a semi-carbene, semi-zwitterion.

Reaction of $\text{HC}\equiv\text{COH}$. In this section, we studied the effect of a hydroxyl group attached to the acetylene moiety. At this time, the structures are labeled with **h** (for $\text{R}_1 = \text{H}$) and **o** (hydroxyl, for $\text{R}_2 = \text{OH}$). The labels **1** and **2** are used as in the methyl case.

Once again, the addition has been found to be a two-step process, but in both cases, the rate-determining step is the initial addition. Figure 5 shows that the attack of CO across the substituted carbon via the transition structure **Ohota1** is more favorable, even though it has a shorter $\text{C}\cdots\text{C}$ intermolecular distance (1.59 Å) versus that in **Ohota2** (1.69 Å) (cf. Supporting Information, Figure S1). On the contrary, the attack of CS to the unsubstituted carbon via **Shota2** is more favored. It is remarkable that the $\text{C}\cdots\text{C}$ intermolecular distance becomes now longer than 2 Å in **Shota2** (Supporting Information, Figure S2). It is also interesting to notice

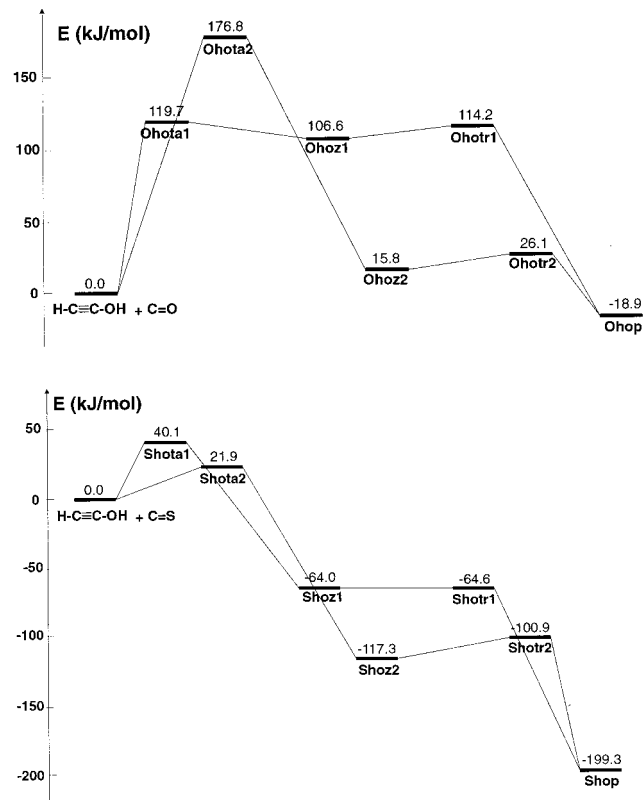


Figure 5. Schematic potential energy profiles for the two-step addition of CX (X = O, S) to $\text{HC}\equiv\text{COH}$. Relative energies obtained at B3LYP/6-311G(d,p) using B3LYP/6-311G(d,p)-optimized geometries and corrected for zero-point contributions.

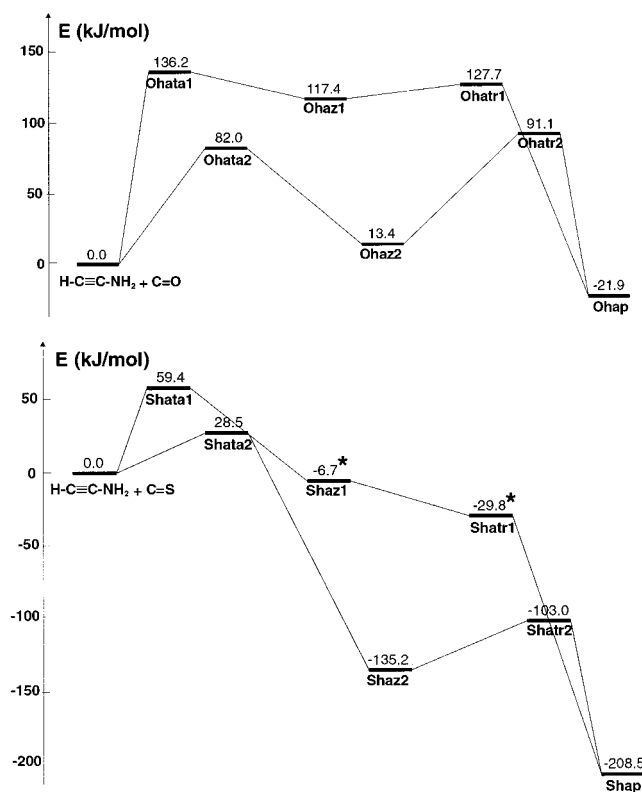


Figure 6. Schematic potential energy profiles for the two-step addition of CX (X = O, S) to HC≡CNH₂. Relative energies obtained from B3LYP/6-311G(d,p) + ZPE calculations. *B3LYP/6-311G(d,p) values using HF/6-31G(d) optimized-geometries and corrected for zero-point contributions.

in Figure 5 that all the intermediates **Xhoz2** forming from the attack of CX to the unsubstituted carbon are considerably stabilized as compared to the substituted case. It is due no doubt to the fact that the strong π -donor hydroxyl group attached to the carbene center atom C₂ reduces the π -electron deficiency and therefore stabilizes the singlet carbene. The delocalization of π -electron can be seen from the plot of HOMO of **Ohoz2** (Figure 4).

Overall, the main effect of the hydroxyl group is a stabilization of the intermediate forming from the attack of CX to the unsubstituted carbon, along with a stabilization of the cyclic product.

Reaction of HC≡CNH₂. Amino (NH₂) is also a strong π -donor group, and its effects are expected to be similar to those in the hydroxyl case. For this structure, **h** is used for R₁ = H and **a** (amino) for R₂ = NH₂.

Figure 6 indicates that in both CO and CS cases the attack at the unsubstituted carbon via the transition state for addition **Xhata2** is more favorable. It is clear that the intermediate **Xhaz2** is more stable than **Xhaz1** (as in the hydroxyl case). Note that we were not able to locate **Shaz1** and **Shatr1** at the B3LYP level. To have an idea about the possible location of those structures, we carried out single-point energy calculations using HF/6-31G(d) geometries. In fact, the intermediate located at the Hartree–Fock level becomes higher in energy than the transition state for ring closure. Again, the rate-determining step is the ring closure in the CO case, but **Ohaz2** lies in a rather deep potential well whereas it is the initial addition attack in the CS case. Relative to the unsubstituted acetylene, the energy barrier for the initial attack is reduced considerably in both CO and CS cases.

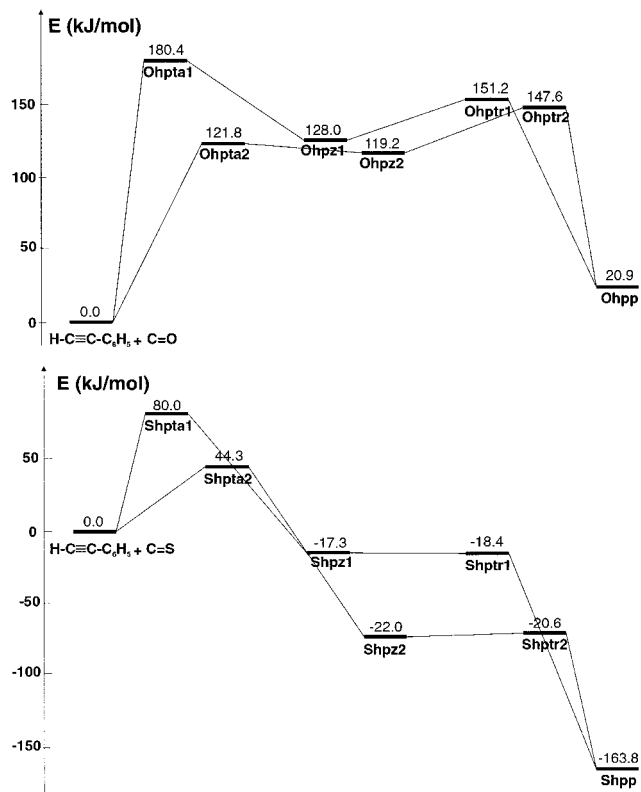


Figure 7. Schematic potential energy profiles for the two-step addition of CX (X = O, S) to HC≡CC₆H₅. Relative energies obtained at B3LYP/6-311G(d,p) using B3LYP/6-311G(d,p)-optimized geometries and corrected for zero-point contributions.

The C₂–C₃ bond distances in **Xhaz2** are shorter than those in **Xhhz** (1.33 Å in **Ohaz2** and 1.32 Å in **Shaz2** versus 1.36 Å in **Ohhz** and 1.35 Å in **Shhz**) (Supporting Information, Figures S3 and S4). It is similar to the hydroxyl case (1.34 Å in **Ohoz2** and 1.32 Å in **Shoz2**); thus, it is suggested that, in the amino case, the intermediates **Xhaz2** have more properties of a singlet carbene.

Reaction of HC≡CC₆H₅. Here we have chosen the phenyl group (C₆H₅) as an acetylene substituent. In this case, **h** stands for R₁ = H and **p** (phenyl) for R₂ = C₆H₅.

The attack across the unsubstituted carbon is much more favorable either in the addition or the ring formation (Figure 7). It is reinforced by the steric effect of the phenyl group. In the CO case, the rate-determining step is the ring closure and the intermediate **Ohpz2** lies a few kilojoules per mol lower in energy than the corresponding transition structure **Ohpta2**. It is in contrast with the CS case, in which the transition structures for ring-closure lie only about 1 kJ/mol higher in energy than the intermediates. Such difference arises again from the higher exothermicity of the CS addition.

It is also interesting to notice that the (C₁C₂C₆H₅) angles in the intermediates **Xhpsz2** are larger than those in the previous cases (Supporting Information, Figures S5 and S6). Tomioka⁴⁵ and Bourissou et al.⁴⁶ demonstrated that the phenyl group having a conjugating and steric bulk effect will favor the triplet state and broaden

(45) Tomioka, H. *Acc. Chem. Res.* **1997**, *30*, 315.

(46) Bourissou, D.; Guerret, O.; Gabbai, F. P.; Bertrand, G. *Chem. Rev.* **2000**, *100*, 39.

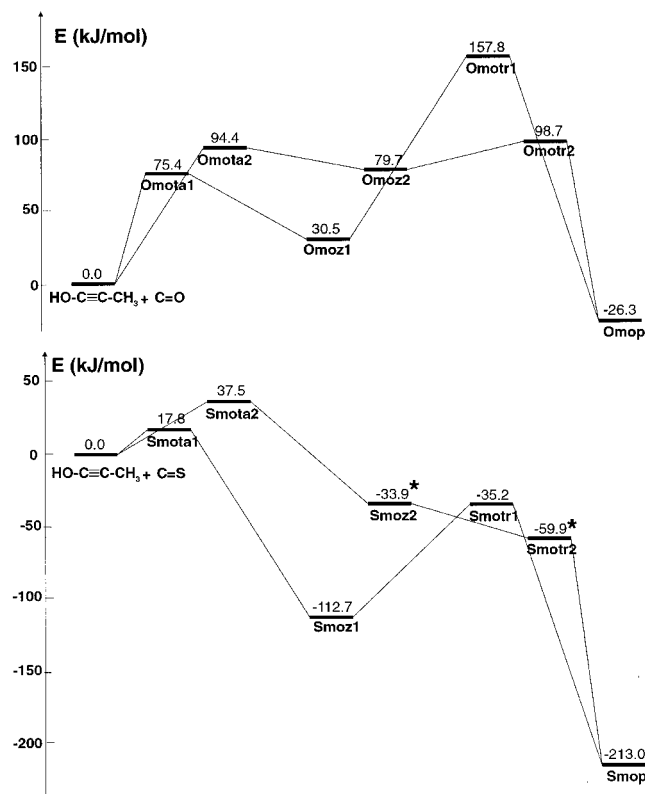


Figure 8. Schematic potential energy profiles for the two-step addition of CX (X = O, S) to $\text{HOC}\equiv\text{CCH}_3$. Relative energies obtained from B3LYP/6-311G(d,p) + ZPE calculations. *B3LYP/6-311G(d,p) values using HF/6-31G(d)-optimized geometries and corrected for zero-point contributions.

the carbene bond angle. Owing to the presence of the CX species, the intermediates **Xhpz2** still exist in the singlet state but their carbene bond angles have increased.

Reaction of $\text{HOC}\equiv\text{CCH}_3$. In this section, we studied the combined effects of substituents. We have selected $\text{HOC}\equiv\text{CCH}_3$ as a simple model system. Here, **o** (hydroxyl) stands for $R_1 = \text{OH}$ and **m** (methyl) for $R_2 = \text{CH}_3$. The label **1** is used for the attack of CX to $\text{C}(-\text{CH}_3)$ and **2** for the attack to $\text{C}(-\text{OH})$.

In both the CO and CS cases, the attack takes place across the CH_3 -substituted carbon via the transition structure **Xmota1** (Figure 8). The ring-closure step is rate determining in the CO case, but it is the initial attack in the CS case. Note that the intermediates **Xmoz1** lie in a deep potential well whereas **Omoz2** is located in a shallow one, and especially, **Smoz2** (and also **Smotr2**) cannot be determined at the B3LYP level.

It is also interesting to look at the structures of the intermediates **Xmoz1** and **Xmoz2** (Supporting Information, Figures S7 and S8). **Xmoz1** has the hydroxyl group attached to the carbene center atom, whereas it is the methyl group in **Xmoz2**. In both the CO and CS cases, **Xmoz1** is more stable than **Xmoz2**. It is well-known that hydroxyl group mesomeric effect strongly stabilizes singlet carbene, whereas methyl group inductive effect does not. The difference in the interaction of OH- and CH_3 -group orbitals with the carbene center can be observed in Figure 4.

Reaction of $\text{HOC}\equiv\text{CC}_6\text{H}_5$. In the last case, we now consider the combination of the hydroxyl and phenyl groups in acetylenes. For this model, **o** (hydroxyl) stands

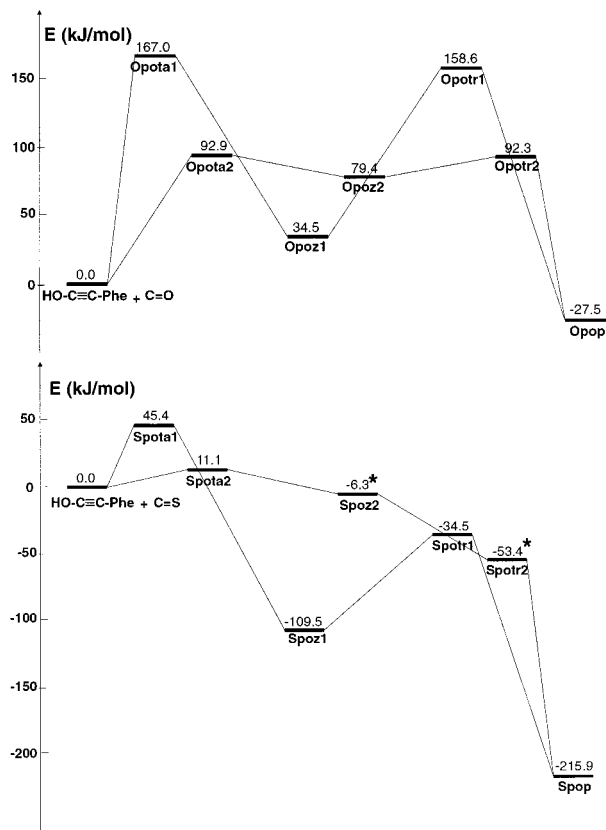


Figure 9. Schematic potential energy profiles for the two-step addition of CX (X = O, S) to $\text{HOC}\equiv\text{CC}_6\text{H}_5$. Relative energies obtained from B3LYP/6-311G(d,p) + ZPE calculations. *B3LYP/6-311G(d,p) values using HF/6-31G(d)-optimized geometries and corrected for zero-point contributions.

for $R_1 = \text{OH}$ and **p** (phenyl) for $R_2 = \text{C}_6\text{H}_5$. The label **1** is used for the attack of CX to $\text{C}(-\text{C}_6\text{H}_5)$ and **2** for the attack to $\text{C}(-\text{OH})$.

In this case, the addition also proceeds in two steps, in which the attack across the OH-substituted carbon via the transition structure **Xpota2** is more favored (Figure 9). The intermediates **Xpoz1**, which have the hydroxyl group attached to the carbene center, lie in a deep potential well, whereas **Opoz2** locates in a shallow one, and **Spoz2** (and also **Spotr2**) cannot be obtained at the B3LYP level. This is no doubt due to the effect on the singlet carbene of the hydroxyl group (Supporting Information, Figures S9 and S10). For its part, phenyl carbene has a stronger tendency to exist in a triplet state than in a singlet state. Again, due to the high exothermicity in the formation of cyclopropenethiones, the rate-determining step is the initial attack in the CS case, whereas in the CO case both addition and ring-closure steps appear to be competitive processes.

Particularly, in this case, to further pursue the observations obtained from the preliminary study on the addition of CX (X = O, S) to $\text{HC}\equiv\text{CH}$,³⁶ we also calculated the single point electronic energies of all the stationary structures in the presence of a solvent continuum including water, acetonitrile, and benzene.

Calculated results performed at the B3LYP/6-311G-(d,p) level and using the PCM model are listed in Table 2. As observed in the previous work,³⁶ the shape of the potential energy surface is not affected by the polarity of the studied solvents. In most cases, increasing the ϵ

Table 2. Relative Energies (kJ/mol) of Related Structures in the Reaction $\text{HOC}\equiv\text{CC}_6\text{H}_5 + \text{CX}$ ($\text{X} = \text{O}, \text{S}$) in the Gas Phase and in Solution Using the PCM at B3LYP/6-311G(d,p)

structure	gas	benzene	acetonitrile	water
	phase	$\epsilon = 2.247$	$\epsilon = 36.64$	$\epsilon = 78.39$
$\text{HOC}\equiv\text{CC}_6\text{H}_5 + \text{CO}$	0.0	0.0	0.0	0.0
Opota1	167.0	165.0	168.3	178.0
Opoz1	34.5	22.5	25.8	32.5
Opotr1	158.6	145.0	143.4	149.3
Opota2	92.9	93.2	96.5	104.3
Opoz2	79.4	74.1	79.1	87.6
Opotr2	92.3	86.5	90.2	97.3
Opop	-27.5	-49.9	-53.7	-53.5
$\text{HOC}\equiv\text{CC}_6\text{H}_5 + \text{CS}$	0.0	0.0	0.0	0.0
Spota1	45.4	45.9	48.0	59.7
Spoz1	-109.5	-116.6	-111.9	-99.5
Spotr1	-34.5	-45.0	-44.9	-34.1
Spota2	11.1	18.5	26.6	46.5
Spoz2	-6.3	-26.6	-23.6	-7.9
Spotr2	-53.4	-68.4	-61.2	-44.3
Spop	-215.9	-235.8	-237.7	-234.9

Table 3. First Vertical Excitation Energies Calculated from CIS/6-311++G(d,p) and TD-B3LYP/6-311++G(d,p) of Related Structures in the $\text{HOC}\equiv\text{CC}_6\text{H}_5 + \text{CO}$ Reaction

structure	ground state rel energy (kJ/mol)	first vertical excitation energies			
		TD-B3LYP/6-311++G(d,p)		CIS/6-311++G(d,p)	
		eV	kJ/mol	eV	kJ/mol
CO		8.4	812.6	9.1	876.1
$\text{HOC}\equiv\text{CC}_6\text{H}_5$		4.8	463.7	5.6	542.8
$\text{CO} + \text{HOC}\equiv\text{CC}_6\text{H}_5$	0				
Opota1	167.0	3.0	293.4	3.8	363.4
Opota2	92.9	3.4	325.1	3.8	363.7
Opoz1	34.5	3.1	301.8	3.6	343.9
Opoz2	79.4	2.2	211.4	2.3	221.1
Opotr1	158.6	2.9	281.8	3.2	309.0
Opotr2	92.3	2.2	213.7	2.2	212.2
Opop	-27.5	4.0	382.4	5.6	541.6

value of the solvent tends to increase the stabilization of the three-membered ring product. On the contrary, increasing the polarity of the solvent leads to a general trend of decreasing the stabilization of all intermediates and transition structures, which have less polar nature than the three-membered ring product. Due to the small activation energy found in many cases for the ring-closure step, the solvent effect is expected to modify the shape of the potential energy surface even with a small variation in solvation energies. However, the energy barriers between the intermediates and transition structures for addition- or ring-closure steps remain almost unchanged regardless the solvent polarity. Thus, the intermediate in the CS addition (**Spoz2**) is unlikely to exist in solvent continuum.

Besides, we also computed the first vertical excitation energies by using the CIS/6-311++G(d,p) and time-dependent density functional theory (TD-B3LYP/6-311++G(d,p)) methods. The results are summarized in Table 3. The same calculations for all studied cyclopropenones and cyclopropenethiones are listed in Table 4.

Accordingly, a larger amount of energy is required to promote an electron to the first excited state as compared to the activation energy and the energy of reaction. Also, the required energy to promote one electron from the ground state of the cyclopropenones and cyclopropenethiones to the first excited state is very high (Table 4). As such, it is reasonable to assume that all the studied reactions on the additions or decompositions are likely

Table 4. First Vertical Excitation Energies Calculated from CIS/6-311++G(d,p) and TD-B3LYP/6-311++G(d,p) of Studied Cyclopropenones and Cyclopropenethiones

structure	first vertical excitation energies			
	TD-B3LYP/6-311++G(d,p)		CIS/6-311++G(d,p)	
	eV	kJ/mol	eV	kJ/mol
Ohap	5.0	479.3	6.5	629.8
Ohmp	4.2	409.0	6.1	587.7
Ohop	4.9	476.0	6.5	625.5
Ohpp	3.3	321.6	5.6	537.9
Omop	5.0	478.3	6.7	641.8
Spop	2.7	260.6	4.5	431.2
Shap	3.5	333.1	4.6	442.5
Shmp	3.3	315.8	4.4	420.6
Shop	3.4	325.5	4.5	432.3
Shpp	2.4	226.8	4.4	420.5
Smop	3.5	341.3	4.6	447.7

to take place in the ground electronic state rather than in an excited state. These results confirm our observations in the preliminary work.³⁶

Effects of Substituents on the Aromaticity of Cyclopropenones and Cyclopropenethiones. As mentioned in the Introduction, the question of whether cyclopropenones are aromatic is not well answered yet. Recently, on the basis of the geometric, energetic, charge density, and magnetic criteria (magnetic susceptibilities and NMR chemical shifts), Burk et al.⁴⁷ proposed that cyclopropenones as well as cyclopropenethiones are remarkably aromatic. In this study, we use a complementary approach, namely the nucleus-independent chemical shifts (NICS), to probe again their aromaticity.

The NICS values defined in the geometric center of the rings and NICS(+1) values obtained at 1 Å above the geometric ring center were calculated by means of the magnetic shielding derived from the gauge-independent atomic orbital (GIAO) method at the B3LYP/6-311G(d,p) level. Since the NICS values in the ring plane contain both the in-plane delocalization of electrons in σ -bonds (σ -aromaticity) and a small part of the π electron delocalization, only NICS(+1) values, largely determined by the cyclic π electron delocalization, are listed in Table 5. The NMR chemical shifts of the protons δ values are also presented in Table 5.

Comparison of the NICS(+1) and δ values of cyclopropenones, cyclopropenethiones, and substituted cyclopropenes to those of benzene shows that all investigated species are aromatic except for the case of 4-silatriafulvene, which is antiaromatic. This conclusion is in agreement with the results obtained from the works of Burk et al.⁴⁷ and Saebø.⁴⁸ It seems that the inductive effect of CH_3 increases the aromaticity of cyclopropenones and cyclopropenethiones, whereas the mesomeric and conjugating effects of OH, NH_2 , F, and C_6H_5 reduce their aromaticity. There is no evidence for a relationship between NICS(+1) values with the NMR chemical shifts δ . As far as we aware, such relation has never been reported in the literature. Moreover, the choice of the position where the NICS value is calculated is still arbitrary and needs to be further studied. Nevertheless, NICS(+1) values seem to be more or less correlated with other criteria such as magnetic susceptibility anisotropy and chemical shifts.⁴⁷

(47) Burk, P.; Abboud, J.-L. M.; Koppel, I. A. *J. Phys. Chem.* **1996**, *100*, 6992.

(48) Saebø, S.; Stroble, S.; Collier, W.; Ethridge, R.; Wilson, Z.; Tahai, M.; Pittman, C. U., Jr. *J. Org. Chem.* **1999**, *64*, 1311.

Table 5. NICS(+1) Values Taken from GIAO/B3LYP/6-311G(d,p) of Cyclopropenones, Cyclopropenethiones and Related Structures

substituents					substituents				
name	R ₁	R ₂	NICS (+1)	δ^a (ppm)	name	R ₁	R ₂	NICS (+1)	δ^a (ppm)
Ohmp	H	CH ₃	-10.00	8.67 (8.66) ^b	Shmp	H	CH ₃	-10.80	8.65
Ohhp	H	H	-9.61	9.26 (9.08) ^c	Shhp	H	H	-10.27	9.12
Omop	OH	CH ₃	-9.21		Shap	H	NH ₂	-10.12	6.69
Ohap	H	NH ₂	-9.17	6.04	Smop	OH	CH ₃	-9.98	
Ohop	H	OH	-9.03	6.56	Shpp	H	C ₆ H ₅	-9.83	8.77
Ohpp	H	C ₆ H ₅	-8.97	8.73	Shop	H	OH	-9.60	7.05
Ohfp	H	F	-8.75	6.86	Sppp	C ₆ H ₅	C ₆ H ₅	-9.37	
Oppp	OH	C ₆ H ₅	-8.15		Spop	OH	C ₆ H ₅	-9.01	
Oppp	C ₆ H ₅	C ₆ H ₅	-8.08		Shfp	H	F	-8.93	7.29
	benzene (3)		-11.13	7.54 (7.26) ^d	methylene cyclopropene (or triafulvene) (6)			-7.83	8.10
	iminocyclopropene (4)		-8.97	8.59	silylenecyclopropene (or 4-silatriafulvene) (7)			9.56	6.84
	phosphenecyclopropene (5)		-8.45	8.71					

^a Relative to TMS. $\sigma^1(\text{H}(\text{TMS}))$: B3LYP/GIAO/6-311G(d,p): 32.023. ^b Experimental value in ref 12a. ^c Experimental value in ref 12b,c. ^d Experimental value in ref 12d.

Table 6. Criteria Used in the Reaction of Substituted Acetylenes and CO^a

structure	global softness (au)	site	E_{act} (kJ/mol)	q_{ESP}^b	q_{NPA}^c	Δ_{ESP}^d	Δ_{NPA}^e	C_1^f (HOMO)	hardness (au)	polarizability (au)	NICS (+1)
HOC≡CC ₆ H ₅	2.952	C1-(R)	167.0	-0.53	-0.14	0.69	0.84	0.41	0.145	107.3	-3.7
		C2-(OH)	92.9	0.32	0.33	1.00	0.67	0.39	0.131	117.8	-6.5
HC≡CC ₆ H ₅	2.895	C1-(R)	180.4	-0.15	-0.02	1.58	1.39	0.29	0.152	100.5	-3.7
		C2-(H)	121.8	-0.33	-0.20	0.23	0.27	0.43	0.129	110.0	-8.3
HC≡CNH ₂	2.354	C1-(R)	136.2	0.34	0.16	2.29	1.20	0.40	0.161	47.5	-7.8
		C2-(H)	82.0	-0.65	-0.33	0.00	0.05	0.63	0.175	45.6	-9.0
HOC≡CCH ₃	2.353	C1-(R)	75.4	-0.22	-0.14	0.18	0.13	0.62	0.179	52.6	-11.0
		C2-(OH)	94.4	0.08	0.29	0.67	0.73	0.47	0.167	54.8	-8.5
HC≡COH	2.214	C1-(R)	119.7	0.33	0.31	1.06	0.79	0.45	0.165	42.9	-8.2
		C2-(H)	176.8	-0.66	-0.38	0.01	0.04	0.64	0.152	43.2	-4.4
HC≡CCH ₃	2.048	C1-(R)	150.3	0.20	0.00	0.81	0.38	0.48	0.161	50.3	-8.2
		C2-(H)	122.5	-0.58	-0.25	0.12	0.20	0.50	0.162	50.6	-10.8
HC≡CF	1.857	C1-(R)	96.4 ^g	0.30	0.42	0.07	0.60	0.53	0.176	38.2	-6.4
		C2-(H)	181.9 ^g	-0.59	-0.39	2.29	0.12	0.63	0.157	37.5	-3.8
HC≡CH	1.856	C	144.3 ^e	-0.28	-0.22	0.21	0.21	0.62	0.165	38.6	-7.6

^a Values in bold italic: the failed cases of the criterion according to the rule of thumb (see text). ^b q_{ESP} : electrostatic potential driven charges (ESP). ^c q_{NPA} : natural population analysis (NPA) charges. ^d Δ_{ESP} : square of the softness differences between C of CO and C₁, C₂ of acetylenes using ESP charges. ^e Δ_{NPA} : Δ values obtained from NPA charges. ^f C 2p coefficients perpendicular to C≡C bond axis taken from HF/STO-3G. ^g Values in ref 36.

Site Selectivity in the Initial Attack of the Addition. The initial attack of CX (X = O, S) to the one or the other of both carbon atoms of a substituted acetylene is not equivalent, leading to two distinct transition structures and to a difference in energy barriers. Thus, it will introduce a regioisomeric mechanism in the initial attack of the addition.

From the analysis of atomic charges (ESP and NPA) listed in Tables 6 and 7, it can be observed that there are more negative charges on the unsubstituted carbon in HC≡CR and on the R-substituted carbon in HOC≡CR. This can be explained either by the hyperconjugation effect (caused by CH₃ group) or the mesomeric effect (caused by the OH, NH₂, F). As discussed in the frontier orbital analysis, CX (X = O, S) behaves as an electrophile and it is expected that this moiety will interact preferentially with the more negatively charged carbon of the acetylenes. The charge analysis clearly fails to predict the site selectivity of some reactions (see Tables 6 and

7) indicating that these reactions are essentially orbital-controlled (cf. § I).

We therefore carried out an analysis using DFT-based reactivity descriptors generalizing the FMO parameters and other criteria not based on atomic charges. The calculated results are also summarized in Tables 6 and 7. Some of the criteria are based on the reactant properties (local softness, global softness, HOMO coefficients), while others are based on the corresponding transition structure properties (activation energy, hardness, polarizability, NICS). Definitions and formulas of DFT-based reactivity descriptors and other criteria^{24,49} and their applications in analyzing the regioisomeric mechanism^{37-43,50} can be found in the literature.

(49) For examples, see: (a) Parr, R. G.; Yang, W. *Annu. Rev. Phys. Chem.* **1995**, *46*, 701. (b) Geerlings, P.; De Proft, F.; Langenaeker, W. *Adv. Q. Chem.* **1999**, *33*, 303. (c) Parr, R. G.; Yang, W. *Density Functional Theory of Atoms and Molecules*; Oxford University Press: New York, 1989.

Table 7. Criteria Using in the Reaction of Substituted Acetylenes and CS^a

structure	global softness (au)	site	E_{act} (kJ/mol)	q_{ESP}^b	q_{NPA}^c	Δ_{ESP}^d	Δ_{NPA}^e	C_i^f (HOMO)	hardness (au)	polarizability (au)	NICS (+1)
HOC≡CC ₆ H ₅	2.95	C1-(R)	45.4	-0.53	-0.14	0.15	0.55	0.41	0.145	126.8	-6.6
		C2-(OH)	11.1	0.32	0.33	0.31	0.41	0.39	0.130	134.2	-5.6
HC≡CC ₆ H ₅	2.90	C1-(R)	80.0	-0.15	-0.02	0.66	1.01	0.29	0.139	122.5	-4.3
		C2-(H)	44.3	-0.33	-0.20	0.00	0.12	0.43	0.127	127.6	-6.0
HC≡CNH ₂	2.35	C1-(R)	59.4	0.34	0.16	1.14	0.85	0.40	0.148	63.7	-5.3
		C2-(H)	28.5	-0.65	-0.33	0.25	0.00	0.63	0.158	60.4	-8.1
HOC≡CCH ₃	2.35	C1-(R)	17.8	-0.22	-0.14	0.00	0.03	0.62	0.165	67.5	-9.3
		C2-(OH)	37.5	0.08	0.29	0.14	0.46	0.47	0.160	69.6	-6.8
HC≡COH	2.21	C1-(R)	40.1	0.33	0.31	0.34	0.51	0.45	0.152	58.9	-5.4
		C2-(H)	21.9	-0.66	-0.38	0.14	0.00	0.64	0.171	53.8	-9.2
HC≡CCH ₃	2.05	C1-(R)	76.3	0.20	0.00	0.20	0.19	0.48	0.145	67.8	-5.8
		C2-(H)	47.2	-0.58	-0.25	0.64	0.07	0.50	0.155	65.2	-8.6
HC≡CF	1.86	C1-(R)	43.1 ^g	0.30	0.42	0.04	0.36	0.53	0.157	53.6	-4.6
		C2-(H)	47.6 ^g	-0.59	-0.39	3.84	0.03	0.63	0.161	52.6	-6.5
HC≡CH	1.86	C	74.4 ^e	-0.28	-0.22	0.00	0.08	0.62	0.147	54.8	-5.6

^a Values in bold italic: the failed cases of the criterion according to the rule of thumb (see text). ^b q_{ESP} : electrostatic potential driven charges (ESP). ^c q_{NPA} : natural population analysis (NPA) charges. ^d Δ_{ESP} : square of the softness differences between C of CS and C₁, C₂ of acetylenes using ESP charges. ^e Δ_{NPA} : Δ values obtained from NPA charges. ^f C 2p coefficients perpendicular to C≡C bond axis taken from HF/STO-3G. ^g Values in ref 36.

As discussed above, CX (X = O, S) will act as an electrophile and substituted acetylene as a nucleophile in reactions under investigation. Therefore, we will consider the local softness for nucleophilic attack (s_k^+) of carbon atom in CX, and for electrophilic attack (s_k^-) of carbon C₁ and C₂ in substituted acetylenes. We define Δ as the square of softness differences between C of CX and C₁, C₂ of substituted acetylenes. From the view of the local HSAB principle,⁵¹ the smaller the Δ value is, the more favorably the initial attack takes place. On the other hand, from the simple consideration of the frontier orbital theory (FMO), the attack of an electrophile will be easier on the atom of its nucleophile partner having larger HOMO coefficient. On the other hand in view of the maximum hardness principle, the minimum polarizability principle, and the considerations about NICS in explaining the regioisomeric mechanism, we expect transition structures having larger hardness, smaller polarizability and larger negative NICS(+1) value at 1 Å above the center of the ring, to be more stable and the reaction path to occur via this transition state.

Overall, we can summarize the combination of all criteria as a rule of thumb as follows: the favored reaction path will take place across the carbon atom of substituted acetylenes having smaller Δ value, larger HOMO coefficient. It also occurs via the transition state (for the initial attack) having smaller activation energy, larger hardness, smaller polarizability and larger negative NICS(+1) values (i.e., higher aromaticity). Note that in each case the hardness-of-the-transition-state criterion is equivalent to an activation hardness criterion (the difference in the hardness of reactants and the hardness of the transition state) as the reactants hardness is identical when studying regioisomeric mechanism.

The observations derived from Tables 6 and 7 are as follows:

In the CO case, the above rule is perfectly respected in the case of HC≡CNH₂ and HOC≡CCH₃. In the attack

Table 8. Failed Cases of Regioisomeric Mechanism Criteria over 14 Studied Cases

criteria	no. of failed cases ^a	failed cases in the attack of	
		CO to	CS to
charges	5 (3)	HOC≡CC ₆ H ₅ HC≡COH HC≡CF	HOC≡CC ₆ H ₅ HC≡CF
Δ_{ESP}	4	HOC≡CC ₆ H ₅ HC≡COH HC≡CF	HOC≡CC ₆ H ₅ HC≡CCH ₃
Δ_{NPA}	3 (1)	HC≡COH HC≡CF HC≡CF	HC≡CF
C _i (HOMO)	5 (3)	HOC≡CC ₆ H ₅ HC≡COH HC≡CF	HOC≡CC ₆ H ₅ HC≡CF
hardness	4 (3)	HOC≡CC ₆ H ₅ HC≡CC ₆ H ₅ HC≡CF	HOC≡CC ₆ H ₅ HC≡CF
polarizability	6 (4)	HOC≡CC ₆ H ₅ HC≡CC ₆ H ₅ HC≡CCH ₃ HC≡CF	HOC≡CC ₆ H ₅ HC≡CF
NICS (+1)	2 (1)		HOC≡CC ₆ H ₅ HC≡CF

^a In parentheses: number remaining after subtracting the HC≡CF case.

of CS, it is the case of HC≡CNH₂, HOC≡CCH₃, HC≡CC₆H₅, and HC≡COH.

The failed cases of all criteria (in bold face in Tables 6 and 7) over 14 cases (the case of HC≡CH + CX is excluded) are listed in Table 8. According to Table 8, there are two cases (HOC≡CC₆H₅ and HC≡CF) in which almost all criteria fail to predict the site for the initial attack. The fluorine substituent is almost an exception in all regioisomeric mechanism studies,^{37,52} and until now, unfortunately, there is no reasonable explanation for this behavior. In general, the evaluation of the regioisomeric mechanism is based on the properties of isolated reactants (charges, softness differences Δ , HOMO coefficient), but obviously other stronger interactions can influence the initial attack sites. For example, the steric bulk effect of the phenyl group can prevent the attack of CX (electrophile) to the carbon C(-C₆H₅) of acetylenes even though this carbon has more negative charge due to the

(50) For examples, see: (a) Ponti, A. *J. Phys. Chem. A* **2000**, *104*, 8844. (b) Pal, S.; Chandrakumar, K. R. S. *J. Am. Chem. Soc.* **2000**, *122*, 4145. (c) Arrieta, A.; Cossio, F. P.; Lecea, B. *J. Org. Chem.* **2000**, *65*, 8458.

(51) (a) Gázquez, J. L.; Méndez, F. *J. Phys. Chem.* **1994**, *98*, 4591. (b) Chattaraj, P. K. *J. Phys. Chem.* **2001**, *105*, 511. (c) Geerlings, P.; De Proft, F. *Int. J. Quantum Chem.* **2000**, *80*, 227.

(52) (a) Chandra, A. K.; Nguyen, M. T. *J. Comput. Chem.* **1998**, *19*, 195; *J. Phys. Chem. A* **1998**, *102*, 6181. (b) Ghanty, T. K.; Ghosh, S. K. *J. Phys. Chem.* **1996**, *100*, 12295.

conjugating effect of the phenyl group. On the other hand, the failed cases of hardness and polarizability criteria also prove that the principle of maximum hardness and the principle of minimum polarizability (which transition structure having higher hardness or lower polarizability will be more stable) could not be applied in all cases. These principles need to be further investigated to give more detailed conditions for a proper application. Among those criteria, it is interesting to note that the NICS(+1) seems to be a good one in explaining the regioisomeric mechanism. To remove the arbitrariness of the point where the NICS is evaluated, we tried to locate the ring critical point on the transition structures for addition. However due to the large distance between the C atom of CO and one of the C atom in the acetylenes, this point was not recognized as such by the program. Subtracting the fluorine case, NICS(+1) values fail only in the CS + HOC≡CC₆H₅ case. Only a single exception (CO + HC≡COH) is then also noticed for the local softness difference when applied with the NPA charges.

For the initial addition giving rise to an intermediate, its stability can also serve as a criterion for selectivity. As demonstrated above, the intermediate is a semi-carbene, semi-zwitterion. Thus any substituent stabilizing the singlet carbene moiety is expected to stabilize the intermediate and as a consequence induce its formation or in other words, it induces an initial addition at the other carbon site of acetylene. This is the case of strong π -donor groups that stabilize carbene. Nevertheless, this consideration does also not explain the regioisomeric mechanism of HOC≡CC₆H₅ and HC≡CF.

Conclusions

In this study, we have demonstrated that the [2 + 1] cycloaddition of CX (X = O, S) to acetylenes proceeds in two steps: addition of CX to a carbon atom of acetylenes giving rise to an intermediate, followed by a ring-closure step of the latter to form at last cyclopropanones or cyclopropanethiones. In all cases, CX behaves as an electrophile and acetylenes as nucleophiles. For both CO and CS attacks, the intermediate structure is best described as a resonance hybrid between a carbene and a zwitterion. In the CO case, most of the intermediates, transition structures and three-membered ring products lie higher in energy than the reactants (CO + R₁C≡CR₂). It is in contrast to the CS case where all corresponding intermediates and products lie much lower in energy

than the separated systems (CS + R₁C≡CR₂). Moreover, the energy barriers for the initial attack are not so high, especially in the CS case they are much smaller than those in the CO case. Considering the favored reaction path, for each substituents, the energy barriers will decrease in the order H (144 kJ/mol) > CH₃ > C₆H₅ > OH > F > NH₂ (82 kJ/mol) in the CO case and H (74 kJ/mol) > CH₃ > C₆H₅ > F > NH₂ > OH (22 kJ/mol) in the CS case. A combination of substituents tends to stabilize the intermediates and further reduces the energy barriers.

The studied solvents tend to stabilize all the isomers of the HOC≡CC₆H₅ system. In other systems, due to the flatness of the potential energy surface around the intermediates, their existence appears to be unlikely in solvent continuum. From this work, it is also shown that the promotion of an electron from the ground state of studied molecules to an excited state requires a large amount of energy. As such, all investigated reactions are expected to take place in the ground-state rather than in an excited state.

It is also proved especially via the NICS(+1) values as well as the calculated and experimental NMR chemical shifts that all studied cyclopropanones, cyclopropanethiones and related cyclopropanes are more or less aromatic. The [2 + 1] cycloadditions are clearly orbital controlled and the softness differences Δ based on the properties of isolated reactants is valid in predicting the site of the initial attack, whereas only NICS seems to be a good criterion among those based on the corresponding transition structures. The stability of the carbene intermediate also constitutes a simple criterion for the regioisomeric mechanism of the initial addition.

Acknowledgment. We are grateful to the FWO Vlaanderen (VUB) and a GOA program (KUL) for financial support and to the VUB computer center for helping with our calculations.

Supporting Information Available: Figures showing the geometrical parameters along the reaction path in the reaction of CX (X = O, S) + HC≡COH (Figures S1 and S2), CX + HC≡CNH₂ (Figures S3 and S4), CX + HC≡CC₆H₅ (Figures S5 and S6), CX + HOC≡CCH₃ (Figures S7 and S8), and CX + HOC≡CC₆H₅ (Figures S9 and S10). Z-matrices or Cartesian coordinates with the computed total energies for all studied structures. This material is available free of charge via the Internet at <http://pubs.acs.org>.

JO015584H